Geotechnical and Geophysical Site Characterization 4 – Coutinho & Mayne (eds)

Use of the Seismic Dilatometer (SDMT) to estimate in situ G-γ decay curves in various soil types

S. Amoroso & P. Monaco
University of L'Aquila, Italy

D. Marchetti
Marchetti, Rome, Italy

ABSTRACT: This paper illustrates the use of the Seismic Dilatometer (SDMT) to assess the in situ decay of stiffness with strain level (G-γ curves or similar) in different soil types. The approach adopted in this study relies on the ability of the SDMT to provide routinely at each test depth both a *small strain* stiffness (G_0 from V_S) and a *working strain* stiffness (constrained modulus M_{DMT} from usual DMT interpretation). At various test sites *working strain* DMT moduli (G_{DMT} or E_{DMT}, derived from M_{DMT} by elasticity theory) have been compared with same-depth reference stiffness decay curves back-figured from the observed behavior under a full-scale test embankment (Treporti) or footings (Texas), obtained by laboratory tests (L'Aquila) or reconstructed by combining different in situ/laboratory techniques (Western Australia). Typical ranges of the shear strain γ_{DMT} associated to G_{DMT} in different soil types have been inferred from the intersection of the DMT data points with the reference stiffness decay curves.

1 INTRODUCTION

The seismic dilatometer (SDMT) is the combination of the flat dilatometer (DMT) with an add-on seismic module for the measurement of the shear wave velocity V_S.

This paper is aimed at investigating the possible use of the SDMT to estimate in situ decay curves of soil stiffness with strain level (G-γ curves or similar), suitable to describe with reasonable accuracy the non-linear pre-failure soil behavior.

Methods for deriving G-γ curves from in situ tests have been proposed by various Authors (e.g. Robertson & Ferrera 1993 and Fahey 1998, from U/R cycles of the self-boring pressuremeter; Mayne et al. 1999 and Marchetti et al. 2008, from SDMT; Elhakim & Mayne 2003 and Mayne 2003, from the seismic cone SCPT; Lehane & Fahey 2004, from SCPT and DMT).

The approach adopted in this study relies on the ability of the SDMT to provide routinely, at each test depth, both the stiffness at *small strains* (the small strain shear modulus G_0 obtained from the shear wave velocity V_S as $G_0 = \rho V_S^2$) and the stiffness at *operative strains* (as represented by the constrained modulus M_{DMT} obtained by the usual DMT interpretation). Such two stiffness values may offer guidance when selecting the G-γ curves, i.e. the decay of the shear modulus G with the shear strain γ.

2 SEISMIC DILATOMETER TEST (SDMT)

The seismic dilatometer (SDMT) is the combination of the mechanical flat dilatometer (DMT), introduced by Marchetti (1980), with an add-on seismic module for measuring the shear wave velocity V_S. First introduced by Hepton (1988), the SDMT was subsequently improved at Georgia Tech, Atlanta, USA (Martin & Mayne 1997, 1998; Mayne et al. 1999). A new SDMT system (Fig. 1) has been recently developed in Italy (Marchetti et al. 2008).

The seismic module (Fig. 1a) is a cylindrical element placed above the DMT blade, equipped with two receivers spaced 0.50 m. The shear wave source, located at ground surface, is an automatic hammer or a pendulum hammer (≈10 kg) which hits horizontally a steel rectangular plate pressed vertically against the soil (by the weight of the truck) and oriented with its long axis parallel to the axis of the receivers, so that they can offer the highest sensitivity to the generated shear wave. When a shear wave is generated at the surface (Fig. 1b), it reaches first the upper receiver, then, after a delay, the lower receiver. The seismograms acquired by the two receivers, amplified and digitized at depth, are transmitted to a PC at the surface, which determines the delay. V_S is obtained as the ratio between the difference in distance between the source and the two receivers (S_2–S_1) and the delay of the

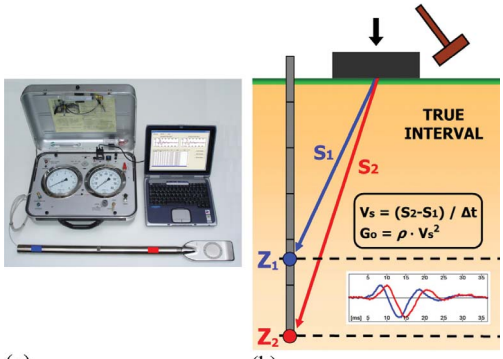

Figure 1. Seismic dilatometer test: (a) SDMT equipment (blade and seismic module); (b) Schematic test layout.

arrival of the impulse from the first to the second receiver (Δt).

The determination of the delay from SDMT seismograms, normally obtained using a cross-correlation algorithm rather than relying on the first arrival time or specific single points in the seismogram, is generally well conditioned. The *true-interval* test configuration with two receivers avoids possible inaccuracy in the determination of the "zero time" at the hammer impact, sometimes observed in the *pseudo-interval* one-receiver configuration. Moreover, the couple of seismograms recorded by the two receivers at a given test depth corresponds to the same hammer blow and not to different blows in sequence, which are not necessarily identical. Hence the repeatability of V_S measurements is considerably improved (observed V_S repeatability ≈1 %, i.e. a few m/s). V_S measurements are taken every 0.50 m of depth (while the mechanical DMT readings are taken every 0.20 m). Validations of V_S measurements by SDMT by comparison with V_S measured by other in situ seismic tests at various research sites are reported by Marchetti et al. (2008). Besides the shear wave velocity V_S, the SDMT provides the parameters obtained from the usual DMT interpretation, e.g. the constrained modulus M_{DMT} (Marchetti 1980, TC16 2001).

3 TENTATIVE METHOD FOR DERIVING IN SITU G-γ DECAY CURVES FROM SDMT

Research in progress, outlined by Marchetti et al. (2008), investigates the possible use of the SDMT for deriving "in situ" decay curves of soil stiffness with strain level (G-γ curves or similar). Such curves could be tentatively constructed by fitting "reference typical-shape" laboratory G-γ curves (see e.g. Fig. 2, where G is normalized to G_0) through two points, both obtained by SDMT: (1) the initial *small strain* modulus G_0 (obtained as $G_0 = \rho V_S^2$), and (2) a *working strain* modulus G_{DMT}.

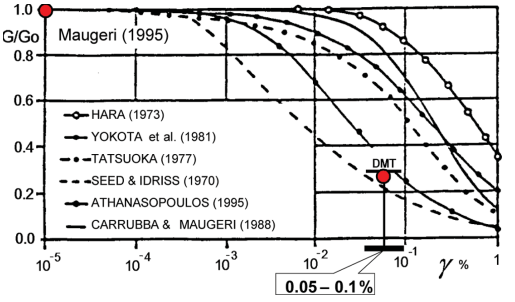

Figure 2. Tentative method for deriving G-γ curves from SDMT (Marchetti et al. 2008).

To locate the second point on the G-γ curve it is necessary to know, at least approximately, the shear strain corresponding to G_{DMT}. Indications by Mayne (2001) locate the DMT moduli at an intermediate level of strain ($\gamma \approx 0.05$–0.1 %) along the G-γ curve. Similarly Ishihara (2001) classified the DMT within the group of methods of measurement of soil deformation characteristics involving an intermediate level of strain (0.01–1 %). The above qualitative indications need to be confirmed by further investigations.

As suggested by Marchetti et al. (2008), a *working strain shear modulus* G_{DMT} can be derived from the constrained modulus M_{DMT} provided by the usual DMT interpretation (Marchetti 1980, TC16 2001). As a first approximation, by referring to linear elasticity:

$$G = \frac{1-22\nu}{2(1-\nu)} M \qquad (1)$$

where ν = Poisson's ratio. E.g. assuming $\nu = 0.2$ (as frequently used), the *working strain shear modulus* may be obtained from Eq. (1) as $G_{DMT} = 0.375\, M_{DMT}$.

The potentiality of the above tentative method is heavily founded on the basic premise that M_{DMT} is a reasonable estimate of the "operative" or *working strain* modulus (i.e. the modulus that, introduced into the linear elasticity formulae, provides realistic estimates of the settlement of a shallow foundation under working loads). This assumption is supported by the good agreement observed in a large number of well documented comparisons between measured and DMT-predicted settlements or moduli (see Monaco et al. 2006; Marchetti et al. 2008).

The next section illustrates the use of the SDMT to assess the in situ decay of stiffness at various test sites, in different soil types, where both SDMT data

and "reference" stiffness decay curves were available. Such stiffness decay curves were: (a) back-figured from the observed behavior under a full-scale test embankment (Treporti) or footings (Texas), (b) obtained by laboratory tests (L'Aquila), or (c) reconstructed by the combined use of different in situ/laboratory techniques (Western Australia). The procedure adopted in all cases is the following:

1. Using SDMT data obtained at the same depth of each available reference stiffness decay curve, a *working strain* modulus G_{DMT} (or E_{DMT}) is derived from M_{DMT} by elasticity theory and normalized to its *small strain* value G_0 (or E_0) derived from V_S.
2. The G_{DMT}/G_0 (or E_{DMT}/E_0) data point is superimposed to the same-depth reference stiffness decay curve, in such a way that the data point ordinate matches the curve.
3. The "intersection" of the G_{DMT}/G_0 (or E_{DMT}/E_0) data point with the stiffness decay curve provides a value of the associated abscissa, i.e. the shear strain γ(or other strain).

4 STIFFNESS DECAY BY SDMT AT VARIOUS TEST SITES

4.1 *Treporti, Venice (Italy)*

At the site of Treporti, Venice (Italy)—typical of the highly heterogeneous, predominantly silty deposits of the Venice lagoon—a full-scale vertically-walled cylindrical test embankment (40 m diameter, 6.7 m height, applied load 106 kPa) was constructed and continuously monitored towards pore water pressures, surface settlements, horizontal and vertical displacements with depth (see Simonini 2004 for details). The Treporti test site was extensively investigated by means of piezocone tests (Gottardi & Tonni 2004), flat dilatometer tests (Marchetti et al. 2004), seismic piezocone tests and seismic dilatometer tests (McGillivray & Mayne 2004), continuous coring boreholes and high quality laboratory tests (Simonini et al. 2006). Significant results of the experimental program at Treporti have already been published by various research groups.

The Treporti embankment research has provided a unique opportunity to investigate the decay of soil stiffness in situ by use of accurate measurements of *local* vertical strains in the soil under the embankment, at 1 m depth intervals, provided by sliding deformeters. Young's moduli E (secant) were back-calculated by Marchetti et al. (2006) at the mid-height of each 1 m soil layer, assuming vertical and radial stress distributions provided by current linear elasticity solutions, from local ε_v measured by the sliding deformeter at the center of the embankment under each load increment during construction (from *small* to *working strains*). Figure 3a shows the progressive reduction of the back-calculated moduli E under increasing load, starting from the initial values E_0 derived by elasticity theory from V_S (G_0) measured by SDMT, assuming $\nu = 0.15$. Such variation should reflect the combined effects—of opposite sign—of the increase in stress and strain level (stiffness should increase with stress and decrease with strain). In order to separate the two effects, the dependence of E on current stress level was taken into account, as a first approximation, by use of the classic Janbu's relation:

$$E = K_E\, p_a\, (\sigma'_v/p_a)^n \qquad (2)$$

where K_E = modulus number, p_a = reference atmospheric pressure (100 kPa), σ'_v = current vertical effective stress, and n = exponent generally varying between 0.5 to 1, assumed = 0.8 (from back-fitting of the observed moduli profiles). The variation of the modulus number K_E corresponding to E back-calculated under each load increment is shown in Figure 3b, which clearly shows the decay of stiffness with increasing strain, even purged of the effects of stress increase.

In situ curves of decay of soil stiffness with strain level were reconstructed by Marchetti et al. (2006), from the back-calculated moduli E shown in Figure 3, at the mid-height of each 1 m soil layer. To account for the effect of varying stress level, such in situ curves (Figure 4) are expressed in terms of variation of the ratio K_E/K_{E0}—where K_E is the modulus number corresponding to E back-calculated for each load increment (Fig. 3b) and K_{E0} is the modulus number corresponding to the

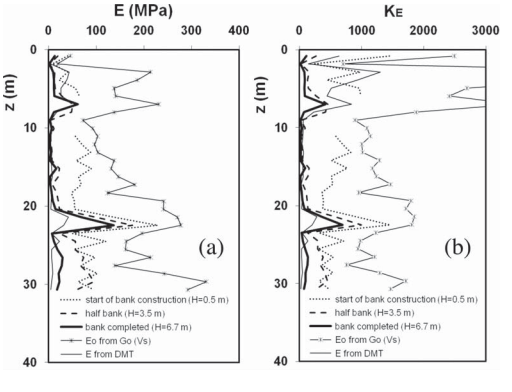

Figure 3. Variation of (a) secant Young's modulus E, and (b) corresponding modulus number K_E, back-calculated from local vertical strains ε_v measured at the center of the Treporti test embankment under various loads throughout construction (after Marchetti et al. 2006).

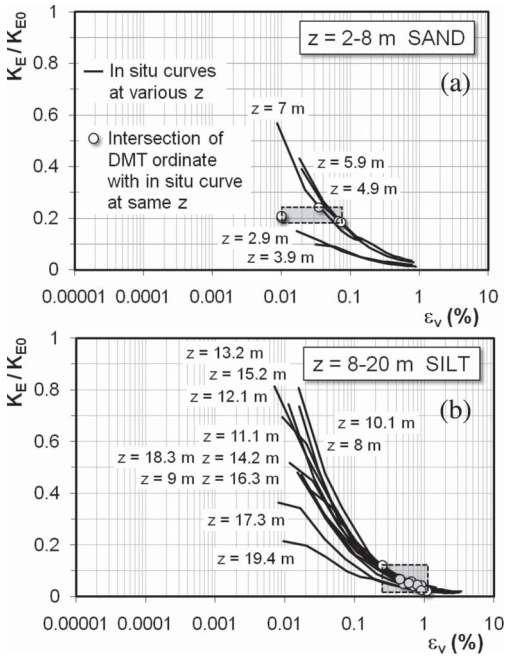

Figure 4. Treporti test embankment—Curves of decay of soil stiffness with vertical strain back-calculated from local ε_v measurements (curves labeled "In situ curves") and their intersection with data points corresponding to same-depth DMT moduli E_{DMT}: (a) in the sand layer 2–8 m depth, and (b) in the silt layer 8–20 m depth (after Marchetti et al. 2006).

initial modulus E_0, obtained by Janbu's expression for $E = E_0$ and $\sigma'_v = \sigma'_{v0}$. The two sets of curves in Figure 4 are representative of distinct soil layers: (a) a sand layer between 2 to 8 m depth, and (b) a silt layer between 8 to 20 m depth (which originated most of the observed settlement, maximum measured $\varepsilon_v \approx 1\%$). (The initial part of the curves in Figure 4 at small strains is missing, since the sliding deformeters did not provide measurements of ε_v less than $\approx 0.5–1 \cdot 10^{-2}$ %).

In Figure 4 the data points corresponding to the DMT moduli E_{DMT} (average values over each 1 m measurement depth interval) are superimposed to the same-depth observed in situ decay curves.

The moduli E_{DMT} were derived from the constrained moduli M_{DMT} using the theory of elasticity (Eq. 3):

$$E_{DMT} = \frac{M_{DMT}(1+\nu)/(1-2\nu)}{(1-\nu)} \qquad (3)$$

where ν = Poisson's ratio (assumed equal to 0.15).

The rectangular shaded areas in Figure 4 denote, for each soil layer, the range of values of the ratio K_E/K_{E0} corresponding to E_{DMT}/E_0. The "intersection" of the DMT data points with the observed in situ decay curves indicates that the DMT *working strain* moduli are located in a range of vertical strains $\varepsilon_v \approx 0.01$ to 0.1 % in sand, ≈ 0.1 to 1 % in silt.

4.2 *Texas A&M University national geotechnical experimentation site*

In 1994 a Spread Footing Prediction Symposium was conducted at the Texas A&M University National Geotechnical Experimentation Site, as part of the ASCE Geotechnical Specialty Conference Settlement '94. Five square footings, ranging in size from 1 to 3 m, were constructed and tested to obtain the complete load-settlement curves (Gibbens & Briaud 1994a). The test site, composed of medium dense silty fine sand, was extensively investigated by in several situ tests (SPT, CPTU, DMT, borehole pressuremeter, Cross-Hole, borehole shear test and step blade test). Laboratory triaxial and resonant column tests were executed on reconstituted samples (Gibbens & Briaud 1994b).

Figure 5 shows the in situ stiffness decay curve reconstructed by Berardi (1999) based on the observed performance of the footings. The Young's modulus E' was back-figured from the observed load-settlement curves by use of a non linear iterative approach. The influence of current stress level was considered "implicit" in the E' values determined over a limited influence depth, assumed as $\approx 1 \div 2\ B$ (B = footing width). In Figure 5 the decay of E', normalized to its initial value E_0, is plotted as a function of the relative displacement w/B % (footing settlement w / width B).

From the results of two DMTs executed at the Texas A&M University test site, Young's moduli E_{DMT} (average values over an influence depth $\approx 1 \div 2\ B$)

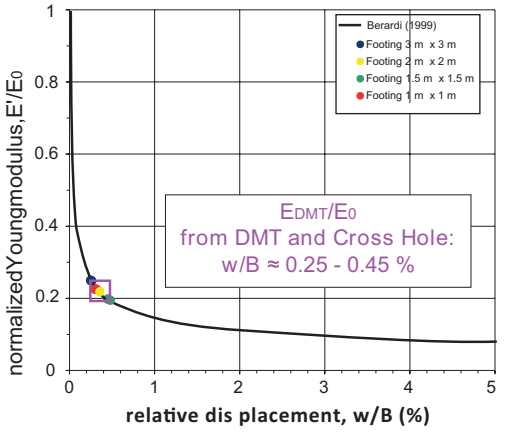

Figure 5. Stiffness decay curve at Texas A&M University National Geotechnical Experimentation Site (Berardi 1999) and superimposed E_{DMT}/E_0 data points.

were derived from M_{DMT} by Eq. (3), assuming $\nu = 0.2$. The initial values of E_0 over the same depth interval were derived from V_S measured by Cross-Hole via elasticity theory (for $\nu = 0.2$). In Figure 5 the data points corresponding to E_{DMT}/E_0 for each footing size (3 m, 2 m, 1.5 m and 1 m) are superimposed to the E'/E_0–w/B curve reconstructed by Berardi (1999). The "intersection" of the DMT data points with the observ ed in situ decay curve indicates that the moduli estimated from DMT are located in a range of relative displacement $w/B \approx 0.25$ to 0.45%.

4.3 *L'Aquila (Italy)*

Following the destructive April 6, 2009 $M_w = 6.3$ earthquake, the area of L'Aquila was extensively investigated by a variety of geotechnical and geophysical testing techniques, involving several working groups. Soon after the earthquake site investigations, including Down-Hole, surface wave tests and SDMT, were concentrated at a number of sites selected for the construction of new temporary houses for the homeless people (C.A.S.E. Project).

Advanced cyclic/dynamic laboratory tests, including resonant column/torsional shear tests (RC–CTS) and double sample direct simple shear tests (DSDSS), were carried out on undisturbed samples from several C.A.S.E. sites, in medium-to fine-grained soils, by a network of Italian soil dynamics laboratories. Details and data are reported in Monaco et al. (2012) and MS-AQ Working Group (2010). The availability of both SDMT and laboratory test results at three C.A.S.E. sites (Cese di Preturo, Pianola, Roio Piano) permitted some calibration of empirical estimates of non-linear parameters from SDMT (Amoroso 2011).

Table 1 reports the values of the shear wave velocity V_S measured by SDMT, the small strain shear modulus G_0 "in situ" obtained from V_S, the constrained modulus M_{DMT} obtained by SDMT at the depth of the samples tested in the laboratory and the *working strain shear modulus* G_{DMT} calculated by Eq. (1), assuming $\nu = 0.2$. The values of the *normalized working strain shear modulus* G_{DMT}/G_0, also reported in Table 1, result 0.10 to 0.23 in silt and clay, 0.37 in silty sand. In Figure 6 each G_{DMT}/G_0 data point (red symbols) is superimposed on the corresponding same-depth laboratory G/G_0 curve (RC tests by University of Napoli Federico II, DSDSS tests by University of Roma La Sapienza). The range of values of the shear strain γ_{DMT} resulting from the "intersection" of the G_{DMT}/G_0 data points with the laboratory curves (rectangular areas in Fig. 6), also reported in Table 1, are $\gamma_{DMT} = 0.24$ to 0.48% in silt and clay, $\gamma_{DMT} = 0.16$ in silty sand.

4.4 *Western Australia*

The G/G_0-γ decay curves presented in this section were obtained at five different test sites in Western Australia (Shenton Park, Ledge Point, Perth CBD, East Perth, Margaret River). Such curves were constructed based on the results of several in situ tests, including flat/seismic dilatometer tests (DMT/SDMT), seismic cone penetration tests (SCPT) and self-boring pressuremeter tests (SBP), and laboratory triaxial tests. Details can be found in Amoroso (2011), Fahey et al. (2003, 2007), Lehane et al. (2007), Lehane (2010), Lehane & Fahey (2004), Schneider et al. (2008), Schneider & Lehane (2010).

The in situ normalized G/G_0-γ decay curves shown in Figure 7 (Shenton Park, silica sand, and Ledge Point, calcareous sand) and in Figure 8 (Perth CBD, alluvial silty clay) were reconstructed

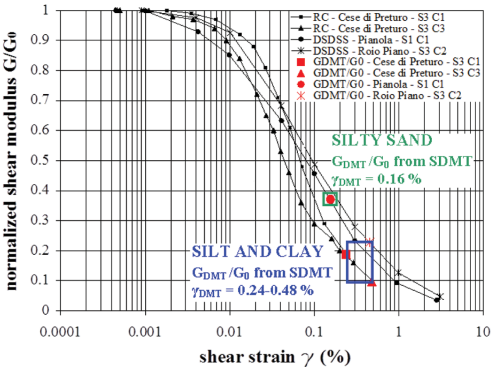

Figure 6. Laboratory G_{DMT}/G_0-γ curves and superimposed G_{DMT}/G_0 data points at three C.A.S.E. project sites, L'Aquila (Amoroso 2011).

Table 1. L'Aquila—Values of G_{DMT}/G_0 obtained from SDMT and corresponding shear strain γ_{DMT} determined from the intersection with the G/G_0-γ laboratory curves at three test sites (Amoroso 2011).

Test site	Sample	Depth (m)	Soil type	V_S (m/s)	G_0 (MPa)	M_{DMT} (MPa)	ν	G_{DMT} (MPa)	G_{DMT}/G_0	γ_{DMT} (%)
Cese di Preturo	S3-C1	4.0–4.8	Silty clay	261	133	67	0.20	25	0.19	0.24
Cese di Preturo	S3-C3	17.5–18.0	Clayey silt	274	149	39	0.20	15	0.10	0.48
Pianola	S1-C1	6.0–6.5	Silty sand	303	195	193	0.20	72	0.37	0.16
Roio Piano	S3-C2	7.0–7.5	Clayey silt	233	105	64	0.20	24	0.23	0.46

by combining the information resulting from SCPT and SBP. In particular:

– the initial part of the curves ($\gamma \leq 0.001\,\%$) was characterized by the small strain shear modulus G_0 obtained from V_S measured by SCPT (no SDMT data were available at these sites);
– the non-linear G/G_0-γ decay at medium to large shear strains ($\gamma \geq 0.01\,\%$) was estimated based on SBP data, according to the procedure proposed by Jardine (1992);
– the central part of the curves ($0.001\% > \gamma > 0.01\%$) was defined by simply connecting the initial part obtained from SCPT (G_0) and the final part obtained from SBP.

The *working strain shear modulus* G_{DMT} was calculated from M_{DMT} obtained by DMT at the same depths of the SCPT and SBP data used to define the G/G_0-γ curve, by use of Eq. (1), assuming $\nu = 0.2$ in sand and $\nu = 0.3$ in silty clay. The values of G_{DMT}/G_0, also reported in Table 2, result 0.08 to 0.31 in

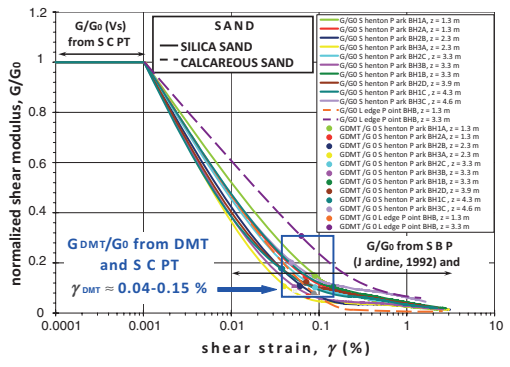

Figure 7. In situ G/G_0-γ decay curves and superimposed G_{DMT}/G_0 data points at Shenton Park and Ledge Point (sand), Western Australia (Amoroso 2011).

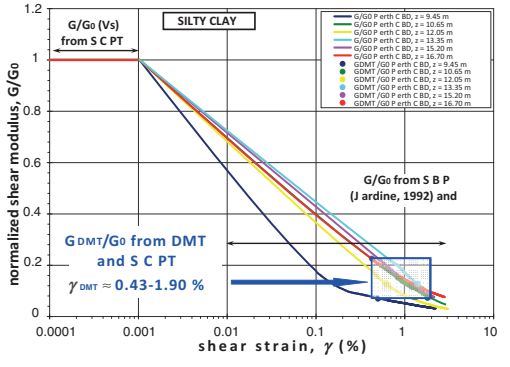

Figure 8. In situ G/G_0-γ decay curves and superimposed G_{DMT}/G_0 data points at Perth CBD (silty clay), Western Australia (Amoroso 2011).

Table 2. Western Australia—Values of G_{DMT}/G_0 obtained from SDMT (or DMT + SCPT) and corresponding shear strain γ_{DMT} determined from the intersection with the G/G_0-γ reference curves at five test sites (Amoroso 2011).

Test site	Borehole or sounding	Depth (m)	Soil type	V_S (m/s)	G_0 (MPa)	M_{DMT} (MPa)	ν	G_{DMT} (MPa)	G_{DMT}/G_0	γ_{DMT} (%)
Shenton Park	BH1A	1.30	Silica sand	252	105	42	0.20	16	0.15	0.09
Shenton Park	BH2A	1.30	Silica sand	252	105	40	0.20	15	0.14	0.07
Shenton Park	BH2B	2.30	Silica sand	267	118	35	0.20	13	0.11	0.06
Shenton Park	BH3A	2.30	Silica sand	267	118	33	0.20	12	0.11	0.04
Shenton Park	BH2C	3.30	Silica sand	280	129	36	0.20	14	0.11	0.15
Shenton Park	BH3B	3.30	Silica sand	280	129	36	0.20	13	0.10	0.09
Shenton Park	BH1B	3.30	Silica sand	280	129	35	0.20	13	0.10	0.05
Shenton Park	BH2D	3.90	Silica sand	282	132	42	0.20	16	0.12	0.07
Shenton Park	BH1C	4.30	Silica sand	283	132	63	0.20	23	0.17	0.04
Shenton Park	BH3C	4.60	Silica sand	283	132	72	0.20	27	0.20	0.05
Ledge Point	BHB	1.30	Calcareous sand	217	78	16	0.20	6	0.08	0.09
Ledge Point	BHB	3.30	Calcareous sand	361	215	176	0.20	76	0.31	0.06
Perth CBD	NML4	9.45	Silty clay	334	212	52	0.30	15	0.07	0.50
Perth CBD	NML4	10.65	Silty clay	373	264	67	0.30	19	0.07	1.80
Perth CBD	NML4	12.05	Silty clay	388	286	130	0.30	37	0.13	0.63
Perth CBD	NML4	13.35	Silty clay	319	193	86	0.30	25	0.13	1.40
Perth CBD	NML4	15.20	Silty clay	324	199	56	0.30	16	0.08	1.90
Perth CBD	NML4	16.70	Silty clay	260	128	101	0.30	29	0.23	0.43
East Perth	BH6	16.00	Soft clay	87	12	1.8	0.20	0.5	0.04	5.50
Margaret River	BH3	6.00	Soft clay	174	55	13	0.20	4	0.07	1.75
Margaret River	BH5	9.00	Silty clay	362	256	68	0.20	20	0.07	0.36

calcareous sand, 0.10 to 0.20 in silica sand, 0.07 to 0.23 in silty clay. The dot symbols in Figures 7 and 8 represent the position of the G_{DMT}/G_0 data points on the corresponding in situ reference G/G_0-γdecay curves. The range of values of the shear strain γ_{DMT} resulting from the "intersection" with the in situ G/G_0-γ curves (shaded areas in Figs 7 and 8), also reported in Table 2, are γ_{DMT} = 0.04–0.15 % in sand and γ_{DMT} = 0.43–1.9 % in silty clay.

The G/G_0 -γ decay curves shown in Figure 9 (East Perth, soft clay) and Figure 10 (Margaret River, silty clay) were reconstructed by combining the information resulting from in situ SDMT and laboratory triaxial tests. In this case:

– the initial part of the curves ($\gamma \leq 0.001$ %) was characterized by G_0 derived from V_S measured by SDMT;
– the non-linear G/G_0 -γ decay at medium to large shear strains ($\gamma \geq 0.1$ % at Margaret River, $\gamma \geq 0.5$ % at East Perth) was estimated from triaxial tests according to Atkinson (2000);
– the central part of the curves (0.001% > γ > 0.5 % at East Perth, 0.001% > γ > 0.1% at Margaret River) was defined by simply connecting the initial part obtained from SDMT (G_0) and the final part obtained from triaxial tests.

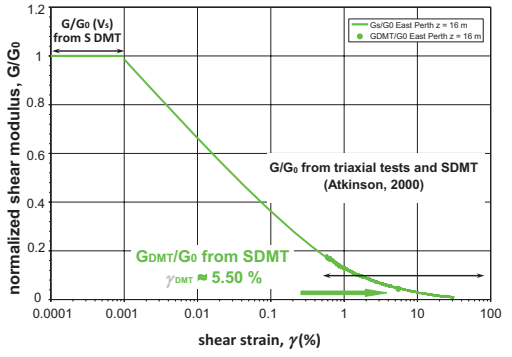

Figure 9. In situ G/G_0-γdecay curves and superimposed G_{DMT}/G_0 data points at East Perth (soft clay), Western Australia (Amoroso 2011).

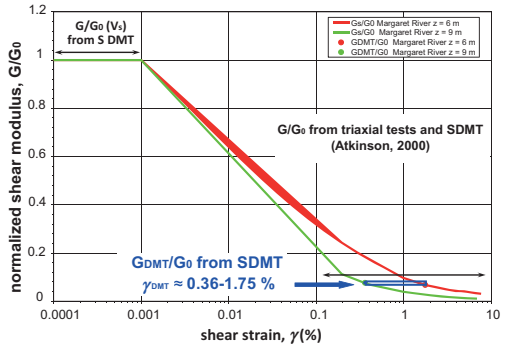

Figure 10. In situ G/G_0-γ decay curves and superimposed G_{DMT}/G_0 data points at Margaret River (silty clay), Western Australia (Amoroso 2011).

The *working strain shear modulus* G_{DMT} was calculated from M_{DMT} obtained by SDMT at the same depths of the samples tested in the laboratory by use of Eq. (1), assuming ν = 0.2 at both sites. The values of G_{DMT}/G_0, reported in Table 2, result 0.04 in soft clay and 0.07 in silty clay. The values of the shear strain γ_{DMT} resulting from the "intersection" of the G_{DMT}/G_0 data points with the reconstructed reference G/G_0-γdecay curves (dot symbols in Figs 9 and 10), also reported in Table 2, are γ_{DMT} = 5.5 % in soft clay and γ_{DMT} = 0.36 to 1.75 % in silty clay.

4.5 *Summary of results at various test sites*

The results obtained at all the test sites previously described are schematically summarized in Figure 11. The shaded areas in Figure 11, superimposed to "typical shape" G/G_0 -γ curves, represent the range of values of the *normalized working strain shear modulus* G_{DMT}/G_0 determined in different soil types (sand, silt and clay, soft clay) and the corresponding shear strain γ_{DMT} determined by the "intersection" procedure. Based on the available information, the "typical range" of shear strain associated to the working strain moduli G_{DMT} can be approximately assumed as: $\gamma_{DMT} \approx$ 0.01-0.45% in sand, $\gamma_{DMT} \approx$ 0.1–1.9% in silt and clay, $\gamma_{DMT} >$ 2% in soft clay.

The above results are in agreement with preliminary literature indications (Mayne 2001, Ishihara 2001). Moreover, the calculated values of the ratio G_{DMT}/G_0—which could be regarded as the shear modulus decay factor at *working strains*—are in line with the trends observed by Marchetti et al.

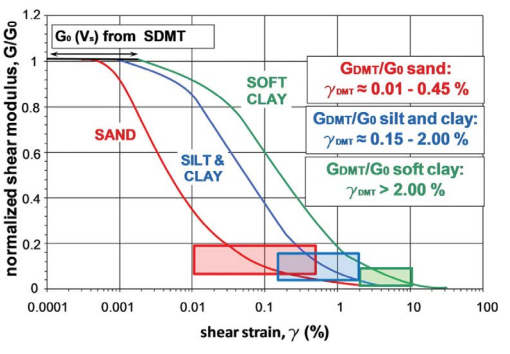

Figure 11. Possible use of the SDMT for calibrating the selection of in situ G/G_0 -γ decay curves in various soil types.

(2008), who investigated the experimental interrelationship between *small strain* and *working strain* stiffness using SDMT in sand, silt and clay. In particular, the diagrams of the ratio G_{DMT}/G_0 vs. the DMT horizontal stress index K_D (related to OCR) constructed by Marchetti et al. (2008) using the SDMT results at 34 different sites, in a variety of soil types, indicated that the G decay in sands is much less than in silts and clays, and that the decay curves in silts and clays are very similar. Also, for all soils the decay is maximum in the NC or lightly OC region (low K_D).

Figure 11 depicts the possible use of the SDMT for calibrating the selection of in situ G/G_0-γ decay curves in various soil types.

5 CONCLUSIONS

The results presented in this paper support the possible use of the SDMT to assess in situ the decay of stiffness with strain level and to address the selection of the G-γ curves in various soil types. This potential descends from the ability of the SDMT to provide routinely, at each test depth, both a *small strain* stiffness (G_0 from V_S) and a *working strain* stiffness G_{DMT} (derived via elasticity theory from the constrained modulus M_{DMT} provided by the usual DMT interpretation). "Reference typical-shape" laboratory G-γ curves may be tentatively fitted through these two stiffness values. A significant premise of this approach is that, to locate the second point on the G-γ curve, it is necessary to know (at least approximately) the shear strain γ_{DMT} corresponding to *working strain modulus* G_{DMT}.

Typical ranges of γ_{DMT} in different soil types have been inferred from the "intersection" of the SDMT data points with same-depth reference stiffness decay curves—back-figured from the observed field behavior under full-scale loading, obtained by cyclic/dynamic laboratory tests or reconstructed by the combined use of different in situ/laboratory techniques—at various test sites.

Based on the available information, typical ranges of γ_{DMT} can be approximately assumed as: $\gamma_{DMT} \approx 0.01$–$0.45\%$ in sand, $\gamma_{DMT} \approx 0.1$–1.9% in silt and clay, $\gamma_{DMT} > 2\%$ in soft clay.

REFERENCES

Amoroso, S. 2011. G-γ decay curves by seismic dilatometer (SDMT). PhD Thesis, University of L'Aquila.

Atkinson, J.H. 2000. Non-linear soil stiffness in routine design. *Géotechnique,* 50(5): 487–508.

Berardi, R. 1999. Non linear elastic approaches in foundation design. In M. Jamiolkowski, R. Lancellotta & D.C.F. Lo Presti (eds), *Pre-failure Deformation Characteristics in Geomaterials*: 733–739. Rotterdam: Balkema.

Elhakim, A.F. & Mayne, P.W. 2003. Derived stress-strain-strength of clays from seismic cone tests. *Proc. 3rd Int. Symp. Deform. Charact. Geomaterials*, Lyon, 1: 81–87.

Fahey, M. 1998. Deformation and in situ stress measurement. In P.K. Robertson & P.W. Mayne (eds), *Proc. 1st Int. Conf. on Site Characterization*, Atlanta, 1:49–68. Rotterdam: Balkema.

Fahey, M., Lehane, B.M. & Stewart, D. 2003. Soil stiffness for shallow foundation design in the Perth CBD. *Australian Geomechanics,* 38(3): 61–90.

Fahey, M., Schneider, J.A. & Lehane, B.M. 2007. Self-boring pressuremeter testing in Spearwood dune sands. *Australian Geomechanics,* 42(4): 57–71.

Gibbens, R.M. & Briaud, J.L. 1994a. Test and prediction results for five large spread footings on sand. *Geotechnical Special Publication No. 41*: 92–128. ASCE.

Gibbens, R.M. & Briaud, J.L. 1994b. Data and prediction request for the spread footing prediction event (at the occasion of the ASCE Spec. Conf. Settlement '94). *Geotechnical Special Publication No. 41*: 11–85. ASCE.

Gottardi, G. & Tonni, L. 2004. A comparative study of piezocone tests on the silty soils of the Venice lagoon (Treporti Test Site). In A. Viana da Fonseca & P.W. Mayne (eds), *Proc. 2nd International Conference on Site Characterization*, Porto, 2: 1643–1649. Rotterdam: Millpress.

Hepton, P. 1988. Shear wave velocity measurements during penetration testing. *Proc. Penetration Testing in the UK*: 275–278. ICE.

Ishihara, K. 2001. Estimate of relative density from in-situ penetration tests. In P.P. Rahardjo & T. Lunne (eds), *Proc. Int. Conf. on In Situ Measurement of Soil Properties and Case Histories*, Bali: 17–26.

Jardine, R.J. 1992. Non-linear stiffness parameters from undrained pressuremeter tests. *Canadian Geotech. Journal,* 29(3): 436–447.

Lehane, B.M. 2010. Shallow foundation performance in a calcareous sand. *Proc 2nd Int. Symposium on Frontiers in Offshore Geotechnics*, ISFOG-2, Perth, 427–432.

Lehane, B.M. & Fahey, M. 2004. Using SCPT and DMT data for settlement prediction in sand. In A. Viana da Fonseca & P.W. Mayne (eds), *Proc. 2nd Int. Conf. on Site Characterization*, Porto, 2: 1673–1679. Rotterdam: Millpress.

Lehane, B.M., Mathew, G. & Stewart, D. 2007. A laboratory investigation of the upper horizons of the Perth/Guildford formation in Perth CBD. *Australian Geomechanics*, 42 (3): 87–100.

Marchetti, S. 1980. In Situ Tests by Flat Dilatometer. *J. Geotech. Engrg. Div.* ASCE. 106 (GT3): 299–321.

Marchetti, S., Monaco, P., Calabrese, M. & Totani, G. 2004. DMT-predicted vs measured settlements under a full-scale instrumented embankment at Treporti (Venice, Italy). In A. Viana da Fonseca & P.W. Mayne (eds), *Proc. 2nd Int. Conf. on Site Characterization*, Porto, 2: 1511–1518. Rotterdam: Millpress.

Marchetti, S., Monaco, P., Calabrese, M. & Totani, G. 2006. Comparison of moduli determined by DMT and backfigured from local strain measurements under a 40 m diameter circular test load in the Venice

area. In R.A. Failmezger & J.B. Anderson (eds), *Proc. 2nd Int. Conf. on the Flat Dilatometer*, Washington D.C.: 220–230.

Marchetti, S., Monaco, P., Totani, G. & Marchetti, D. 2008. In Situ Tests by Seismic Dilatometer (SDMT). In J.E. Laier, D.K. Crapps & M.H. Hussein (eds), *From Research to Practice in Geotechnical Engineering*, *Geotechnical Special Publication No. 180*: 292–311. ASCE.

Martin, G.K. & Mayne, P.W. 1997. Seismic Flat Dilatometer Tests in Connecticut Valley Varved Clay. *Geotech. Testing J.* 20(3): 357–361. ASTM.

Martin, G.K. & Mayne, P.W. 1998. Seismic flat dilatometer in Piedmont residual soils. In P.K. Robertson & P.W. Mayne (eds), *Proc. 1st Int. Conf. on Site Characterization*, Atlanta, 2: 837–843. Rotterdam: Balkema.

Mayne, P.W. 2001. Stress-strain-strength-flow parameters from enhanced in-situ tests. In P.P. Rahardjo & T. Lunne (eds), *Proc. Int. Conf. on In Situ Measurement of Soil Properties and Case Histories*, Bali: 27–47.

Mayne, P.W. 2003. Class "A" footing response prediction from seismic cone tests. *Proc. 3rd Int. Symp. Deform. Charact. Geomaterials*, Lyon, 1: 883–888.

Mayne, P.W., Schneider, J.A. & Martin, G.K. 1999. Small- and large-strain soil properties from seismic flat dilatometer tests. In M. Jamiolkowski, R. Lancellotta & D.C.F. Lo Presti (eds), *Pre-failure Deformation Characteristics in Geomaterials*: 419–427. Rotterdam: Balkema

McGillivray, A. & Mayne, P.W. 2004. Seismic piezocone and seismic flat dilatometer tests at Treporti. In A. Viana da Fonseca & P.W. Mayne (eds), *Proc. 2nd Int. Conf. on Site Characterization*, Porto, 2: 1695–1700. Rotterdam: Millpress.

Monaco, P., Totani, G., Barla, G., Cavallaro, A., Costanzo, A., D'Onofrio, A., Evangelista, L., Foti, S., Grasso, S., Lanzo, G., Madiai, C., Maraschini, M., Marchetti, S., Maugeri, M., Pagliaroli, A., Pallara, O., Penna, A., Saccenti, A., Santucci de Magistris, F., Scasserra, G., Silvestri, F., Simonelli, A.L., Simoni, G., Tommasi, P., Vannucchi, G. & Verrucci, L. 2012. Geotechnical aspects of the L'Aquila earthquake. In M.A. Sakr & A. Ansal (eds), *Special Topics in Advances in Earthquake Geotechnical Engineering*, Chapter 1. Springer Science + Business Media B.V.

Monaco P., Totani G. & Calabrese M. 2006. DMT-predicted vs observed settlements: a review of the available experience. In R.A. Failmezger & J.B. Anderson (eds), *Proc. 2nd Int. Conf. on the Flat Dilatometer*, Washington D.C.: 244–252.

MS–AQ Working Group. 2010. Microzonazione sismica per la ricostruzione dell'area aquilana. Regione Abruzzo—Dipartimento della Protezione Civile, L'Aquila, 3 vol. & Cd-rom (in Italian).

Robertson, P.K. & Ferrera, R.S. 1993. Seismic and pressuremeter testing to determine soil modulus. In *Predictive soil mechanics*, *Wroth Memorial Symposium*: 562–580.

Schneider, J.A., Fahey, M. & Lehane, B.M. 2008. Characterization of an unsaturated sand deposit by in situ testing. *Proc. 3rd Int. Conf. on Site Characterization,* 633–638.

Schneider, J.A. & Lehane, B.M. 2010. Evaluation of cone penetration test data from a calcareous sand dune. *Proc. 2nd Int. Symp. on Penetration Testing*, Huntington Beach, CA.

Simonini, P. 2004. Characterization of the Venice lagoon silts from in-situ tests and the performance of a test embankment. In A. Viana da Fonseca & P.W. Mayne (eds), *Proc. 2nd Int. Conf. on Site Characterization*, Porto, 1: 187–207. Rotterdam: Millpress.

Simonini, P., Ricceri, G. & Cola, S. 2006. Geotechnical characterization and properties of the Venice lagoon heterogeneous silts. *Proc. 2nd Int Workshop on Characterization and Engineering Properties of Natural Soils*, Singapore, 4: 2289–2328. London: Taylor & Francis.

TC16 2001. The Flat Dilatometer Test (DMT) in Soil Investigations—A Report by the ISSMGE Committee TC16. May 2001, 41 pp. Reprint in R.A. Failmezger & J.B. Anderson (eds), *Proc. 2nd Int. Conf. on the Flat Dilatometer*, Washington D.C.: 7–48.